

# Simulating the induction spot welding of hybrid material joints

Mirja Didi, David Wind, Miro Duhovic, , Joachim Hausmann

Institut für Verbundwerkstoffe GmbH, Erwin-Schrödinger-Str., Building 58,  
67663 Kaiserslautern, Germany

## Abstract

Spot welding is a very common process used to join sheet metal components in the automotive industry mass production environment. Recently, thermoplastic composites as lightweight alternatives to metals have begun to make their way into production. The induction spot welding of hybrid materials, in particular aluminum or steel to thermoplastic based composite materials, is one promising method to create the required connections between these dissimilar materials and maintain productivity. As opposed to continuous welding, the spot welding of two materials with different thermal properties can help prevent heat distortion and internal stresses in parts. To improve on the design of the process a deep understanding of the interacting physics of an induction spot welding head is required. A hybrid material spot welding head consists of a stamp, an integrated induction coil and cooling channels. During the process the metal (aluminum) joining partner on the top surface and the fiber reinforced thermoplastic (CF-PA66) on the bottom are fusion bonded to one another via induction heating and pressure. The novel idea of locally concentrating pressure in the fusion zone through a preformed dimple in the metallic joining partner, in order to prevent deconsolidation during induction heating in the thermoplastic adherend, led to noticeably improved joints.

In order to gain a better understanding of this method, the effects of different dimple geometries in the aluminum sheet were reviewed in a simulation utilizing the LS-DYNA® EM Solver. The model considers the mechanical deformation of both metal and composite, the initial micro stresses in the aluminum adherend, thermal convection and radiation, in addition to the electrical conductivity and contact of both joining partners. The model is then used to investigate the temperature, pressure and stresses at the location of the spot weld in order to assess whether an adequate bond has been achieved.

## 1 Introduction

Over the last couple of years, the importance of fiber reinforced plastics (FRP) in industry has grown exponentially. Due to their high strength and low density, these materials are ideally suited for light weight construction. These high performing properties enable manufacturers in many industries to raise efficiency of their products, which - with rising energy prices - is becoming increasingly important. Consequently, fiber reinforced composite materials have secured their placement in many high tech industries, amongst others in automotive, aerospace, medical and mechanical engineering. The market today is mainly dominated by glass, aramid and carbon fibers, which can be combined with numerous thermoplastics and thermosets[1].

Through the targeted use of material combinations, as well as fiber direction and woven structures, almost any material properties for every direction of stress can be designed. Since most technical structures consist of more than one material, an investigation into the suitability of joining techniques for hybrid compounds is crucial.

So far adhesive bonding, laser and induction welding have proven to be successful.[2] This paper further examines the latter, the induction welding process, on the example of aluminum (AlMg3) and carbon fiber reinforced polyamide 66 (CF/PA66). Induction welding is capable of joining both metal to composite as well as composite to composite materials. In the induction welding process electrically conductive or electromagnetic materials are locally heated by induction, until the surfaces intended to be bonded transform into a molten, fusible state. Subsequently, the liquid material solidifies again by cooling and pressure is applied. As a result, the adherends quickly and efficiently fuse together. This joining technology, which has been developed and improved at the Institut für Verbundwerkstoffe GmbH over the last 15 years, exists in two industrially mature processes, today. One is the continuous induction welding; the other is the discontinuous or induction spot welding process. Both processes are highly automatable and yield reproducibly high tensile shear strengths (14.5MPa for AlMg3/CF-PA66 and of 20MPa for DC01/CF-PEEK).[3]

## 2 Principle of induction heating

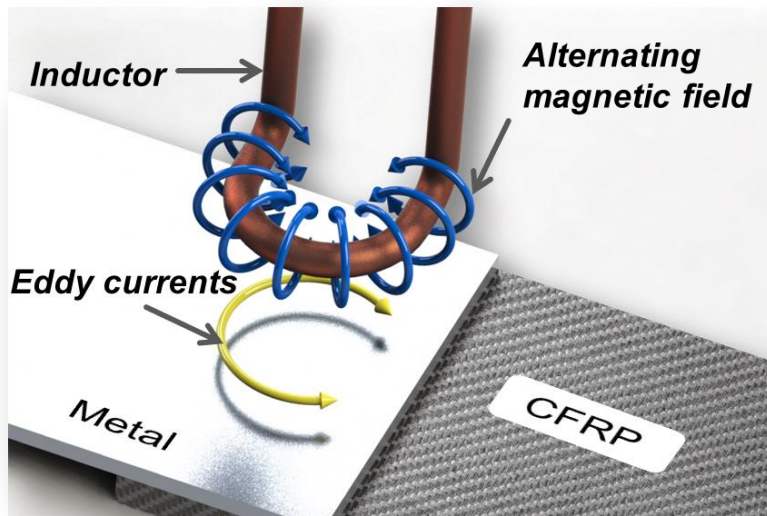


Fig. 1: Principle of induction heating [3].

To achieve the required thermal energy in the welding zone an electric current operating in the kilohertz to megahertz frequency range, supplied by a generator, is applied to a specifically designed coil, called an inductor. The resulting alternating magnetic field surrounding the inductor induces eddy currents in the conductive work piece (see Figure 1) which in turn heats up due to resistive heating or Joule heating or in the case of ferromagnetic materials, magnetic hysteresis. The heat generated by magnetic hysteresis or magnetic polarization is considerably lower than through eddy currents[4]. The amount of heat generated  $Q$  by Joule heating is proportional to the square of the applied current, according to Joule's first law where  $R$  represents the Ohmic resistance and  $t$  the time [5].

$$Q = I^2 R t$$

Since polymers themselves are neither electromagnetic nor electrically conductive and thus do not possess the natural potential for induction heating, the need for an electromagnetic or conductive material in close proximity to the weld location arises. Therefore at least one welding partner needs to consist of a material that matches the aforementioned properties, or a material needs to be added to the welding zone which is capable of absorbing electromagnetic energy and converting it into heat, a so called susceptor [4]. The most commonly used susceptors are metals, metal particles or meshes and carbon fiber reinforced materials. Resistive losses in closed carbon fiber loops of woven reinforcement structures in thermoplastic materials allow for sufficient heating to melt any matrix material by themselves, a process which is then called susceptorless [6]. Once the polymer reaches its melting point in the fusion zone, adhesive forces join the adherends. Due to high processing temperatures and the possibility of deconsolidation, caused by pore formation in the FRP, a stamp or pressure roller with integrated cooling is equally important and provides the necessary force to ensure that the generated heat dissipates allowing the thermoplastic matrix to once again solidify.

## 3 Induction spot welding

The process of induction welding can basically be divided into continuous and discontinuous processes. With continuous induction welding the inductor moves relative to the joining zone, while the necessary consolidation pressure and cooling is applied by a roller traveling behind the inductor.

A major advantage of spot welding over the continuous welding is that an integrated stamp, housing both inductor and cooling system, allows for pressure to be applied during the entire heating phase, thus realizing defined welding spot dimensions through an optimization of the temperature profile. A schematic cross-section of the induction spot welding head developed at the Institut für

Verbundwerkstoffe GmbH and its most important features is shown in Figure 2. This publication focuses on the simulation of induction spot welding using LS-DYNA®.

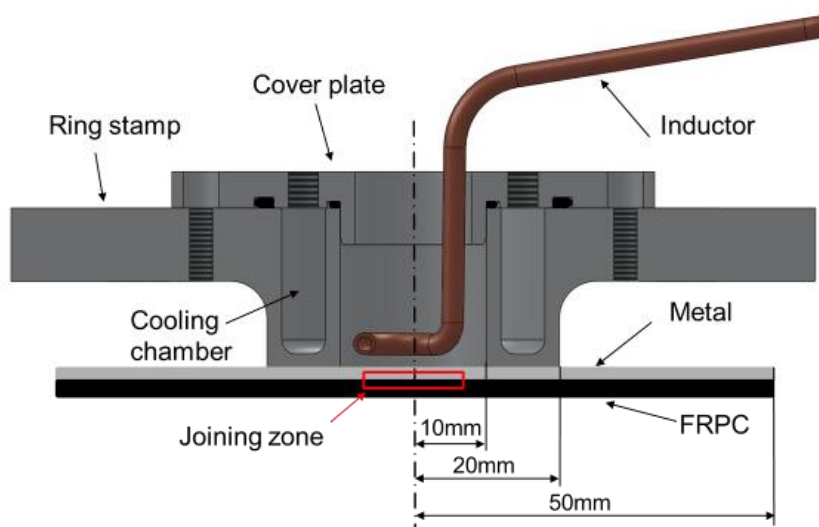


Fig.2: Welding and cooling equipment.

Due to the thermal expansion properties of aluminum and the required geometric restrictions of the stamp (the necessary clearance hole for the inductor and coupling distance), an upwards bulge underneath the inductor is formed reducing the pressure on the composite material in this location. This results in deconsolidation and allows water vapor to form cavities which remain as pores in the fusion zone after the thermoplastic solidifies.

To counteract the problem of uncontrolled bulging of the aluminum during inductive spot welding, the novel idea of prior controlled cold forming of the aluminum blank arose. Here, a defined dimple which can be of various size and depth is cold pressed into the aluminum specimen at the desired weld location; and are then placed, with the bulge facing down, in point contact with the fiber reinforced plastic composite as shown in Figure 3.

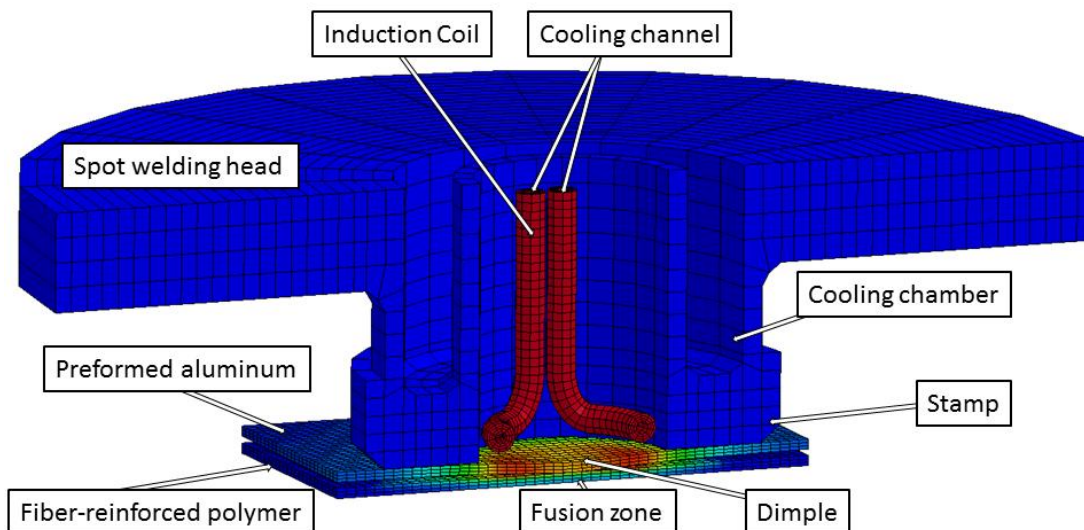


Fig.3: Section view of the induction spot welding process with the preformed aluminum blank.

In contrast to induction spot welding with an undeformed aluminum blank, a more intense and localized heating can be witnessed using a preformed dimple on the aluminum. This is caused by the reduced contact area of the joining partners and the resulting concentration of eddy currents as well as higher contact resistance and heat flow at the contact point. Under the influence of temperature

and pressure, the aluminum is slowly deformed back during the welding process. The contact area between the joining partners gradually becomes bigger and thus more matrix is melted. Ideally, the process finishes with both parts fused and flat against each one another. It is vital to finely tune heating times and the applied pressure in order to achieve a good quality weld. Additionally, even slight variations of different parameters e.g. frequency and power, coupling distance and geometry of the inductor, size, thickness, conductivity and thermal properties of work piece materials directly influence the reproducibility of the process and have a significant impact on the overall results.

Because of this, the numerous parameters, the time consuming cost intensive testing and the general complexity of this technology, development and improvement of this process relies heavily on the inherent advantages of finite element simulations.

#### 4 Finite element simulation of cold deformation of aluminum blank

A device (see Figure 4) was designed and manufactured to cold form the aluminum blanks, utilizing an existing hydraulic workshop press. The device can hold various punch geometries and corresponding dies and allows for aluminum specimens ranging in thickness from 0.5 to 4mm to be indented with a dimple measuring ~20mm in diameter. By applying a force between 10kN and 45kN different dimple depths between 0.5-4mm could be realized.



Fig.4: Components of the device for cold forming of sheet metal specimen [7].

Attention was paid to not decrease the sheet thickness of the blank during forming by testing various punch forces.

While the experimental setup is only capable of controlling the penetration depth of the punch by force, the process of dialing in the required forming force without decreasing the thickness of the blank can only be achieved by trial and error. With the assistance of a finite element simulation set up, in-depth knowledge of the entire process could be gained. In the simulation, the penetration depth of the punch can easily be displacement controlled. The force readouts can then be used to finely tune the preparation process for each experimental specimen. Figure 5 shows as an example, the FEA simulation outputs which define the starting geometry and pre-stresses on the aluminum plates used for investigating spot welding with different dimple heights on a 1mm thick plate.

The entire process is modelled in LS-PrePost® using rigid shell elements for the punch, die and binder components and fully integrated S/R solid elements for the blank. The contacts are defined using `*CONTACT_FORMING_ONE_WAY_SURFACE_TO_SURFACE_SMOOTH` with the master side assigned to the binder and the punch and the slave side to the blank. Due to the high frequency dynamics of the simulation a viscous damping coefficient of 0.2 was used. Shooting node logic was skipped by setting `SNLOG` to 1 in order to gain the correct contact force readouts [8]. The motion of the punch was

imposed using the `*BOUNDARY_PRESCRIBED_MOTION_RIGID` keyword with the velocity defined by `*DEFINE_CURVE_SMOOTH`. The constant binder load is applied via `*LOAD_RIGID_BODY`. To include finite strain data in the binary plot database the option `STRFLG` was set to 1 in `*DATABASE_EXTENT_BINARY` [8]. Through simulation virtually any blank dimension and dimple geometry can be accurately predicted in only a few minutes.

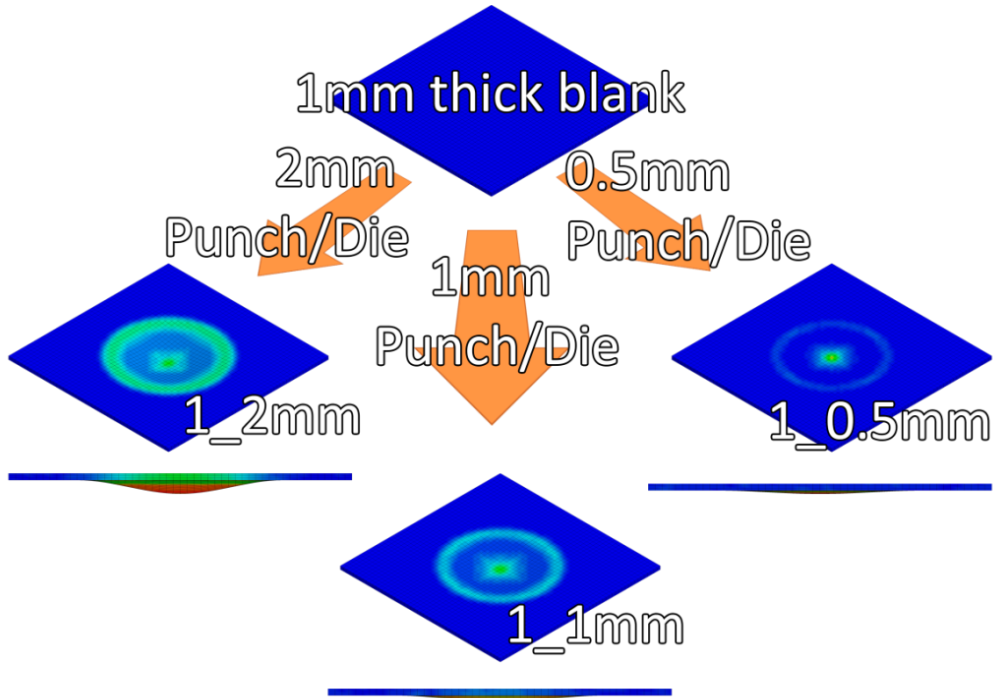


Fig.5: Preparation principle of aluminum preforms 1mm in thickness.

## 5 Finite element simulation of spring-back

Due to the elastic-plastic deformation of the sheet, a geometric change is expected when the part is released from the forming tool. Because of this, the resulting deformed blanks were transferred into an implicit spring-back simulation via `*INTERFACE_SPRINGBACK_LSDYNA`. Figure 6 shows a selection of spring back results for different punch depths on a 0.5mm thick aluminum plate.

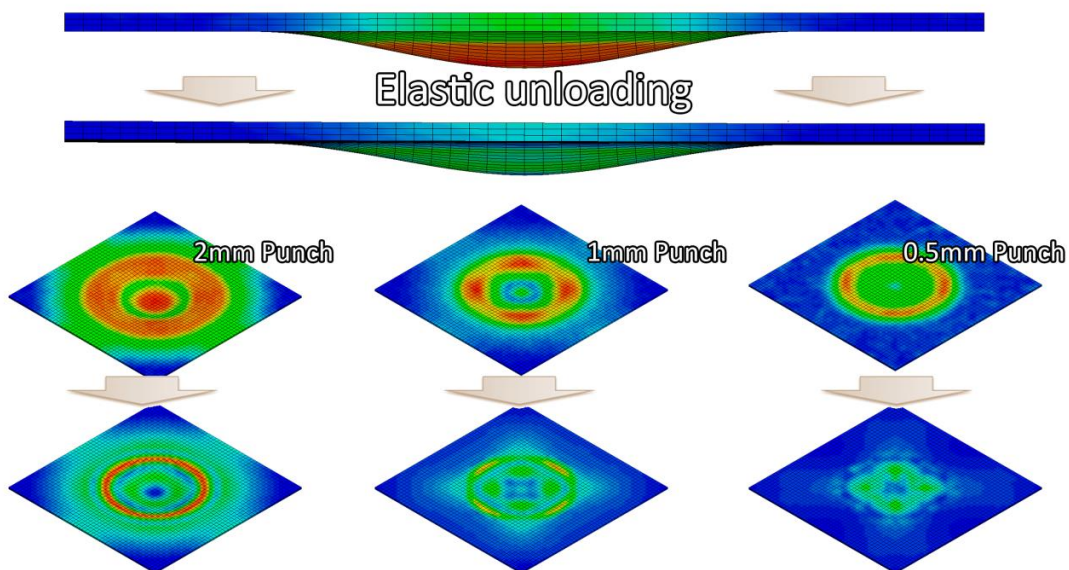


Fig.6: Contours of effective stress in cold formed 0.5 mm thick aluminum plates before and after implicit spring back simulation using different punch depths.

Since the tools have been removed and the sheet is no longer in equilibrium the aluminum unloads its elastic energy stored in the part. The results obtained with the implicit spring back simulation match very well the real world specimens.

## 6 Finite element simulation of the entire induction spot welding process

The model necessary to correctly describe this complex process needed to consider structural, thermal and electromagnetic interactions, while allowing flexible interchangeability of work pieces and material properties. In the following sections, the modelling approach used with LS-DYNA® and some of its considerable advantages are described.

The model consists of an inductor, a stamp with integrated cooling, the preformed aluminum plate and the FRP plate. So far, the electromagnetism solver of LS-DYNA® requires all conducting parts to be modelled with hexahedral solid elements.

The inductor geometry, which is in the shape of a single loop coil, was created via LS-PrePost®'s Shell\_Sweep element generation tool. The stamp consists entirely of hexahedral elements and was generated using tubal Butterfly\_Blocks with the Block\_Mesher. This was then transformed to fit the actual geometry of the water cooled stamp. The inductor and the stamp, both defined as **\*MAT\_020\_Rigid**, are coupled through the **\*CONSTRAINED\_RIGID\_BODIES** keyword so that the inductor maintains a constant coupling distance when the stamp translates and displaces the work piece due to the applied **\*LOAD\_RIGID\_BODY** or stamping force.

For the carbon fiber reinforced Polyamide 66 (CF/PA66) composite plate, both structural and thermal material cards are defined with orthotropic properties based on manufacturer datasheets and experimental analyses performed at the Institut für Verbundwerkstoffe GmbH.

The Aluminum plate, which has already undergone the initial cold deformation and then spring back simulation, is placed in between stamp and FRP plate and contains all residual stress-strain information. Throughout this multi stage simulation, the same material model was used. Due to the asymmetric heating pattern of the coil as well as the edge effect, symmetry could not be used to reduce the required calculation effort.

The model considers three forms of heat transfer: conduction, convection and radiation. Thermal radiation to the environment is considered by applying several **\*BOUNDARY\_RADIATION\_SET** keywords to the surface areas of the objects to be examined. Therefore, a thermodynamic temperature scale where zero degrees must correspond to absolute zero is prerequisite. The Kelvin temperature scale meets this requirement. [9] The fringe plot can easily be offset to the Celsius scale afterwards in the output by using the following commands:

```
fringevariable add a "temperature" 25 2 -1 0 -1 0  
fringevariable fringe "a-273.15"
```

Convection boundary conditions to simulate temperature losses are applied through the card **\*BOUNDARY\_CONVECTION\_SET**. The heat transfer coefficient versus temperature is given as a function in the parameter HLCID and is based on experimental data. The default EM solver EMSOL=1, the Eddy current solver, would be far too resource heavy when using an AC current frequency close to 1MHz and a termination time of several seconds at the same time [10]. Additionally, since Joule heating accounts for most of the energy in this kind of spot welding, EMSOL=2 the induced heating solver is much better suited for this application.

In Figure 7 the principle of the induced heating solver is illustrated. During a 'micro' EM time step, a full Eddy Current problem is solved over one full current oscillation period. An average of the EM fields and Joule heating energy during this period is computed. After reaching a 'macro' time step, a new cycle is initiated with a full Eddy Current resolution. No further EM calculation is performed over the 'macro' time step and the Joule heating is simply added to the thermal solver at each thermal time step [10].

Therefore, in simulations which consider temperature dependent material properties such as heat capacity, thermal and electrical conductivity or where movements are carried out by conductors, a compromise between duration and accuracy of the simulation has to be made when determining the EM 'macro' time step (`*EM_CONTROL_TIMESTEP`).

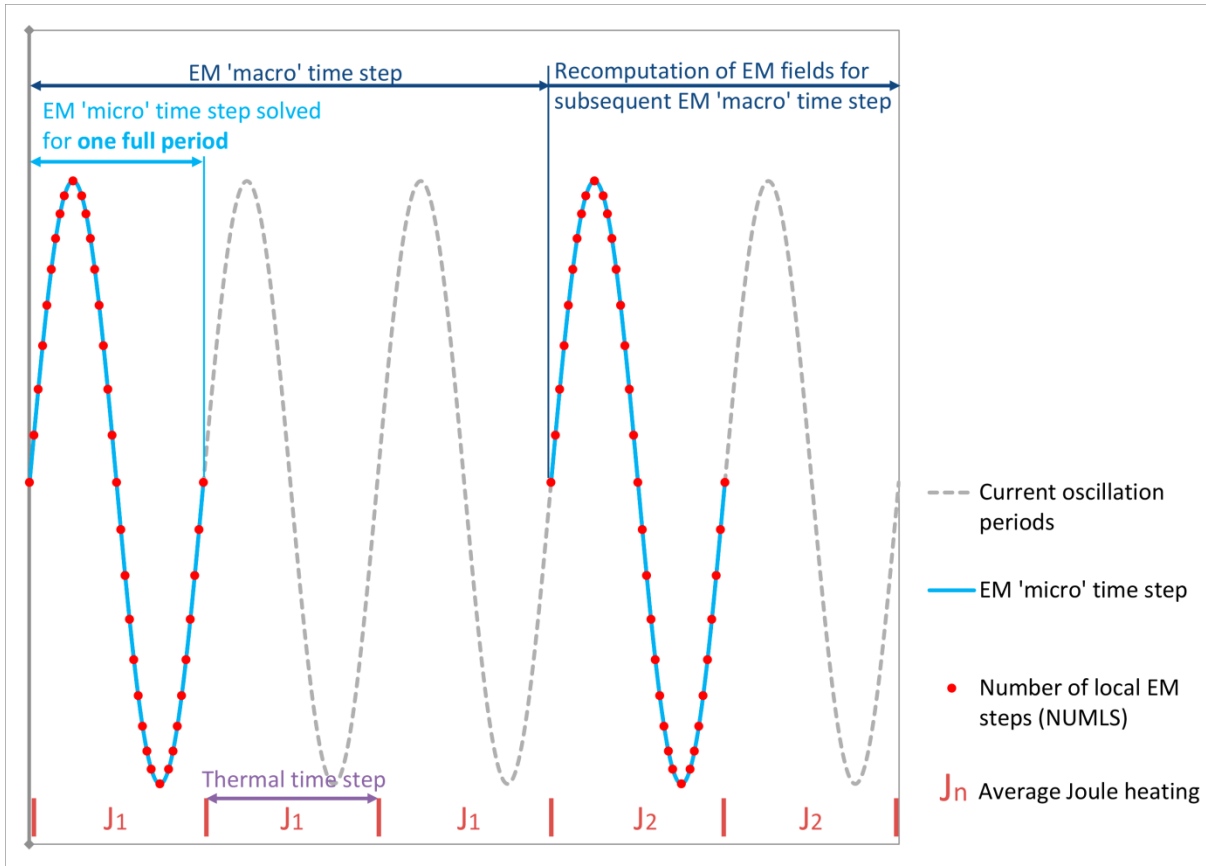


Fig.7: The principle of the inductive heating solver [10].

With the R8 solver, LS-DYNA® allows for electrical contact resistance phenomena to be accounted for in induction heating simulations. Through the card `*EM_CONTACT`, the electromagnetism contact algorithm is activated which detects contact between conductors [9]. Setting the JHRTYPE to 1 in the `*EM_CONTACT_RESISTANCE` card adds the calculated Joule heating evenly to all the elements adjacent to the contact surface. The cards `*EM_DATABASE_CIRCUIT` and `*EM_DATABASE_CIRCUIT0D`, while resource heavy, provide useful additional information.

One of the first discoveries made through the simulation of the induction spot welding process is that a quicker, more locally concentrated heating can be achieved by preserving the integrity of the dimple until thermal bonding begins to occur. First, a contact pressure is applied via the stamp and the dimple is in point contact with the FRP. The Joule heating is then concentrated into this area, which can be observed in the `em_circuitRes_0000X.dat` file output by the `*EM_DATABASE_CIRCUIT` card.

The need for recalculating the EM fields arises as the dimple on the aluminum plate deforms and increased consolidation or phase transitioning takes place. The following diagram shown in Figure 8 schematically explains how the EM time step is intimately connected with the spot welding mechanism taking place in reality and in the simulation.

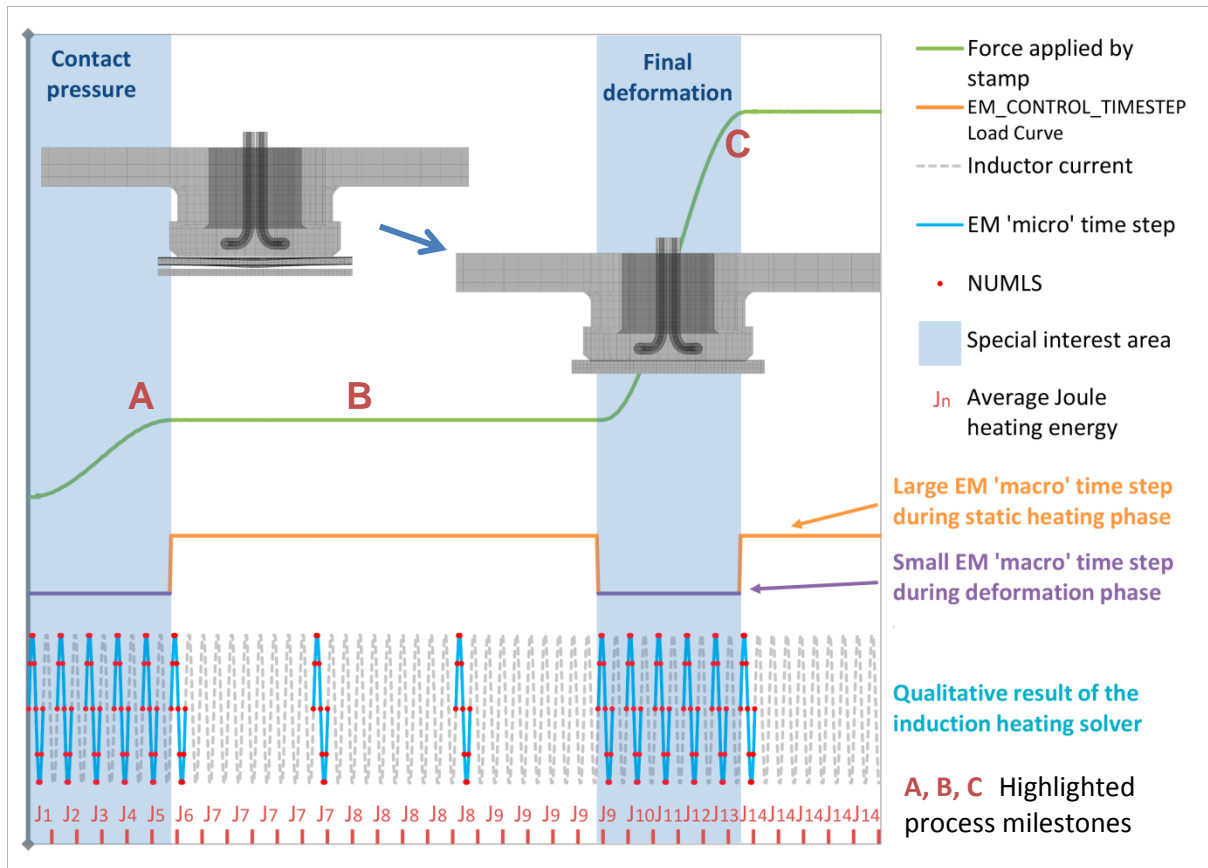


Fig.8: Schematic view of the process sequence and link between the EM time step and the spot welding mechanism taking place.

The process in Figure 8 can be subdivided into 4 parts. First, contact pressure is applied to the preformed aluminum by the stamp. The force applied to the stamp is chosen to be high enough to prevent the FRP from deconsolidating, and thus the formation of pores in the laminate, while not being high enough to entirely deform the aluminum plate back into its original shape and so preserve the geometry of the dimple. In the second step, constant pressure is applied and since only minor deformations are expected, the EM time step is generously increased. The contact area between the two adherends is now statically heated through the Joule heating induced by the inductor. Once the melting temperature of the matrix material in the FRP is reached, the second and final pressing of the stamp is initiated in the third step. In the fourth and final step, the inductor is switched off and the thermoplastic matrix cools and solidifies while still being subjected to the pressure applied by the stamp. The theoretically achieved weld quality can be estimated, based on the temperature and pressure readouts provided by LS-DYNA® available in the binary files, and by analyzing these particular quantities in the contact area.

## 7 Results

Figure 9 shows the developed temperature versus time curves for different through thickness locations in both the aluminum and CF/PA66 plates. It can be seen that as a result of the high thermal conductivity of the aluminum, a homogeneous through thickness temperature distribution is achieved and all curves A–D lay on top of one another. In the CF/PA66 plate however, this is not the case and a large temperature spike is observed at points E and F due to the contact resistance.

In Figure 10, it can be seen that a clear advantage in heating rate and magnitude is gained by having the dimple in addition to the benefits it provides in terms of consolidation and thermal expansion control in the fusion zone. This can perhaps be attributed to the contact resistance and the fact that only a point contact in the heating phase of the process is present and therefore avoids the spread of heat generated at the CF/PA66 and the spot weld interface through the aluminum.

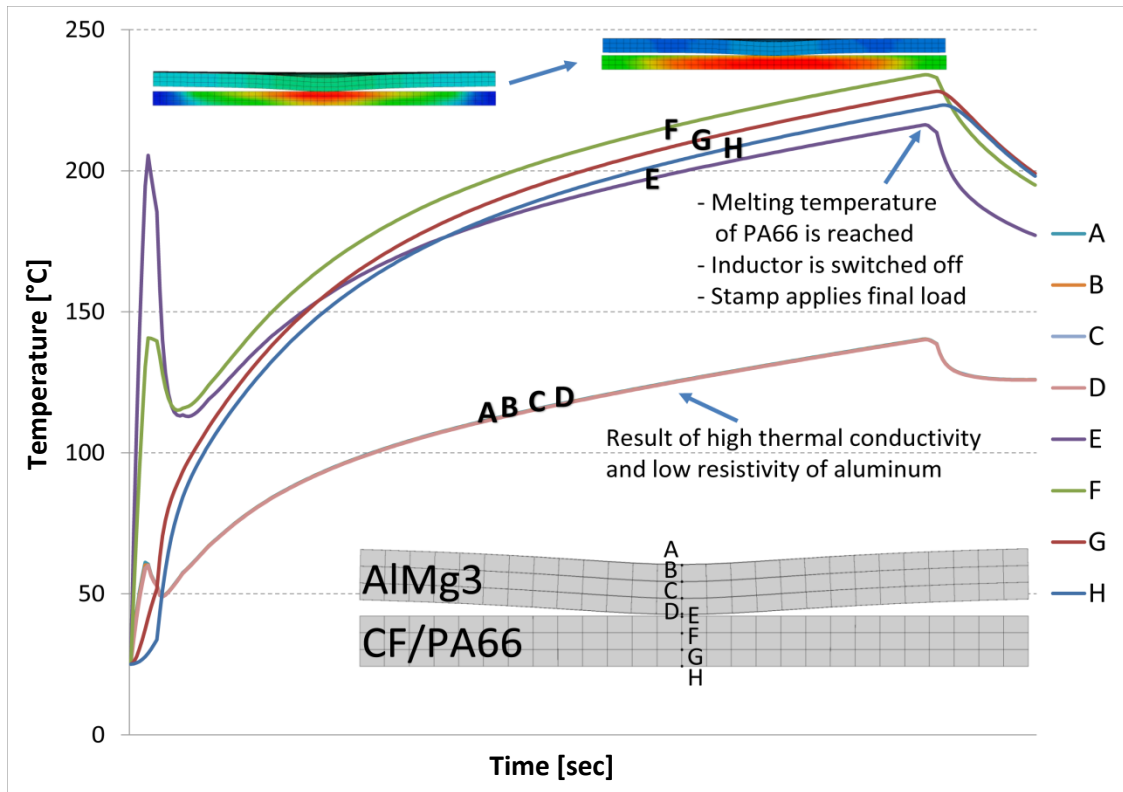


Fig.9: Through thickness temperature profile of 2mm to 2mm spot weld with 1mm deep dimple geometry.

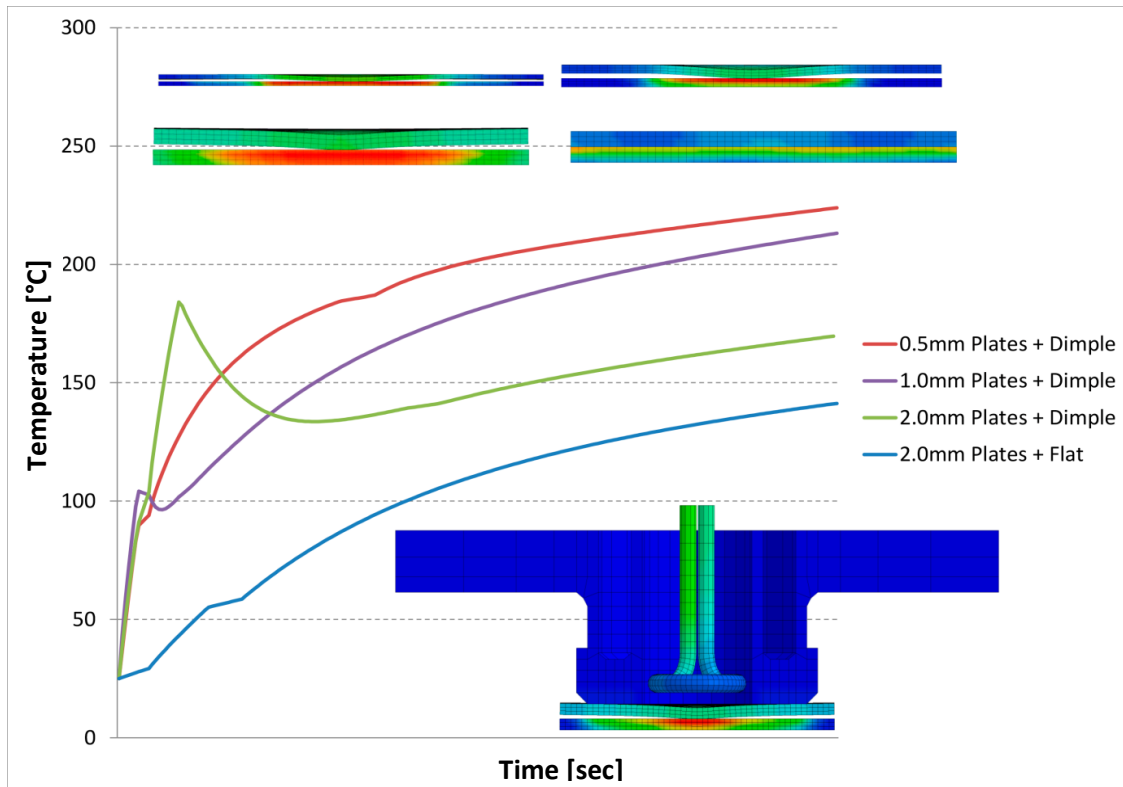


Fig.10: Comparison of average heating rates in the fusion zone for different thickness plates, with and without a spot weld dimple.

Another important aspect of the process is to be able to predict and visualize the temperature distribution within the defined welding area. Figure 11 shows the temperature development after 5, 20

and 70 seconds heating time and demonstrates that the developed welding head can provide a homogeneous temperature over the desired spot weld area.

### Temperature distribution in the weld interface at times **A**, **B** & **C**

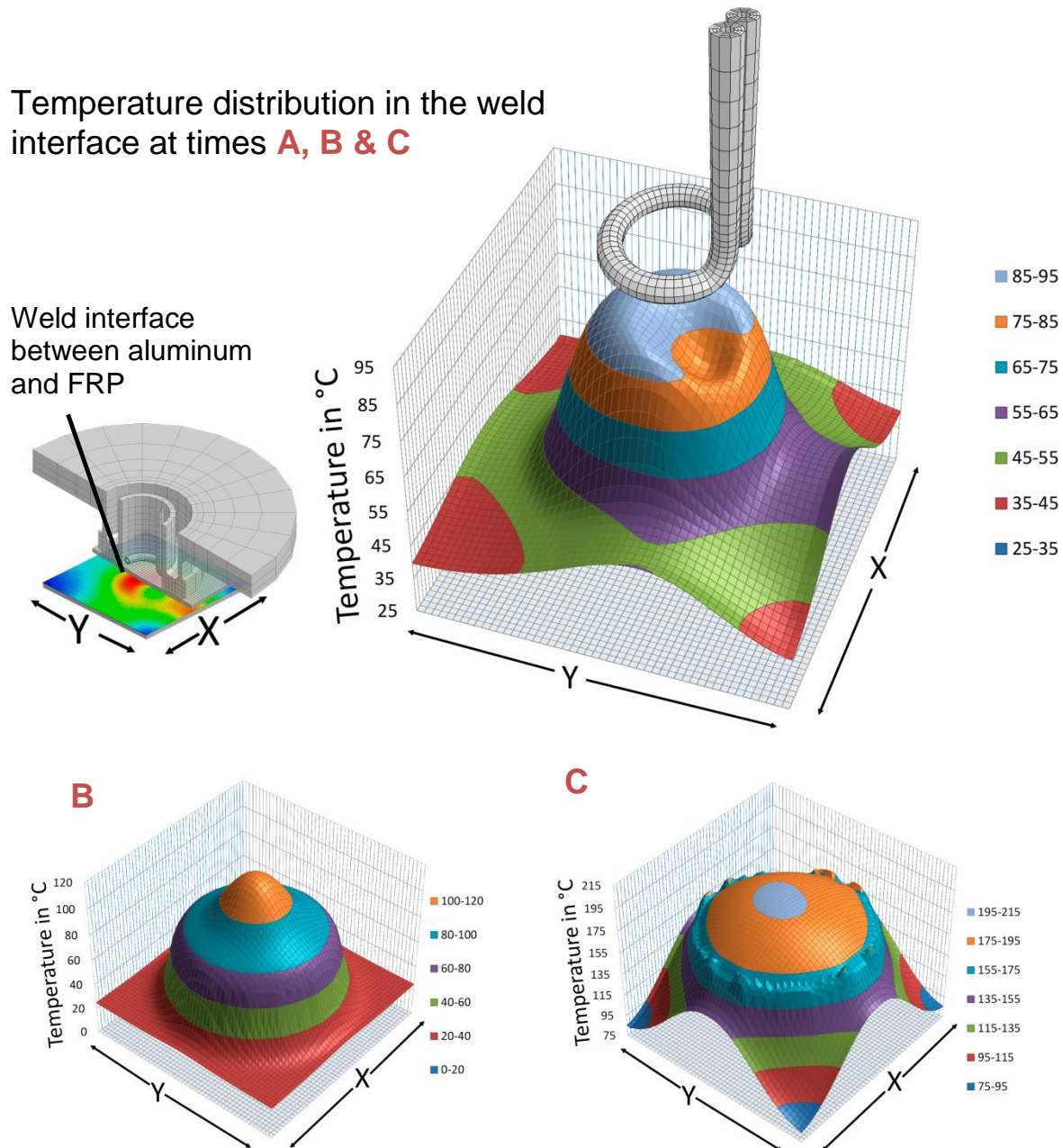


Fig.11: Thermal contour plots at process stages **A** (5sec), **B** (20sec) and **C** (70sec) for the case of a 1 mm thick aluminum plate and 1 mm deep dimple geometry.

## 8 Conclusion

Due to the general complexity of the induction spot welding process and its myriad of parameters, the employment of an advanced multi-physics finite element model to further assist the experimental investigations, was necessary. Within this study, a finite element model of the induction spot welding process was developed which considers structural, thermal and electromagnetic behavior. The LSDYNA® R8 solver has proven to be capable of such complex coupled multi physics simulations enabling the evaluation of different plate and dimple geometries on the induction spot welding of AlMg3 to CF/PA66. It has been shown via simulation, that dimples in the aluminum plate provide significant advantages in terms of heating in addition to assisting the consolidation during the spot welding procedure. The numerical simulations have delivered crucial insights into the complex procedures which would otherwise, in an experimental only setup, require heavy costs and time consuming efforts.

## 9 Acknowledgments

The authors would like to thank Dominic Schommer (IVW), Pierre l'Eplattenier and İñaki Çaldichoury at LSTC for their help and support during the course of this work.

## 10 Literature

1. Bernhard Jahn, E.W. *Composites Market Report 2013*. 2013. 4,19.
2. Manfred Neitzel, P.M., *Handbuch Verbundwerkstoffe Werkstoffe, Verarbeitung, Anwendung*2004, München u.a.: Hanser. XV, 440 S.
3. P. Mitschang, R.V., M. Didi, *Induction spot welding of metal CFRPC hybrid joints*. 2013.
4. V. Rudnev, D.L., R. Cook, M. Black, *Handbook of induction heating*2003.
5. Holm, R., *Die technische Physik der elektrischen Kontakte*. Technische Physik in Einzeldarstellungen1944, Ann Arbor, Mich.: Edwards Bros. x, 337, p.
6. T.J. Ahmed, D.S., H.E.N. Bersee, A. Beukers, *Induction welding of thermoplastic composites – an overview*. Composites Part A, 2006( 37): p. pp. 1638–1651.
7. Tobias Rupp, M.D., *Optimierung eines Werkzeugs zur Herstellung vorgeformter Blechteile*, in *Institut für Verbundwerkstoffe GmbH*2014, Universität Kaiserslautern.
8. Bradley N. Maker, X.Z., *Input Parameters for Metal Forming Simulation*. 2012.
9. Dev, L.-D., *LS-DYNA® KEYWORD USER'S MANUAL Vol. III*. 2014.
10. Pierre l'Eplattenier, I.C. *Electromagnetism Module Presentation*.